

# Temperature dependence of the conductance of multiwalled carbon nanotubes

E. Graugnard\*

*Department of Physics, Purdue University, W. Lafayette, Indiana 47907*

P. J. de Pablo

*Department Física de la Materia Condensada, Universidad Autónoma de Madrid, 28049-Madrid, Spain*B. Walsh<sup>†</sup>, A. W. Ghosh, and S. Datta*Department of Electrical and Computer Engineering, Purdue University, W. Lafayette, Indiana 47907*

R. Reifengerger

*Department of Physics, Purdue University, W. Lafayette, Indiana 47907*

(Received 14 December 2000; published 10 September 2001)

We report on the conductance of multiwalled carbon nanotubes as a function of voltage and temperature between room temperature and 4.2 K. The data show a monotonic decrease in conductance as the temperature is lowered. At temperatures below about 20 K, a nonlinearity develops in the  $V(I)$  data, corresponding to a pronounced dip in the conductance near zero bias. The size of the dip increases as the temperature is lowered. The data are explained in terms of transport through a Luttinger liquid. The measured conductance contains contributions from the nanotube-contact interface and from the nanotube itself.

DOI: 10.1103/PhysRevB.64.125407

PACS number(s): 73.63.Fg, 73.22.-f

## I. INTRODUCTION

It has been found that the conductance of carbon nanotubes displays a pronounced temperature dependence. For single-walled carbon nanotubes (SWNT's) this behavior was explained in terms of the Luttinger liquid (LL) model,<sup>1-3</sup> and supported by theoretical predictions for metallic SWNT's based on their one-dimensional (1D) electronic structure.<sup>4-6</sup> Multiwalled carbon nanotubes (MWNT's) are also predicted to display Luttinger liquid behavior.<sup>7</sup> But so far, the conductance measurements made by Langer *et al.* and Schönenberger *et al.* on MWNT's have shown evidence for either Luttinger liquid behavior or weak localization.<sup>8,9</sup>

Here we report the results of a systematic study of the transport properties on MWNT's. The temperature and voltage dependence of the conductance of MWNT's is measured as a function of temperature between 300 K and 4.2 K. We have used a fabrication technique that produces low-resistance contacts to the nanotube. An analysis of the low-temperature data reveals two contributions which must be taken into account: (i) the LL contact resistance and (ii) the intrinsic conductance of the MWNT.

## II. EXPERIMENTAL CONSIDERATIONS

The MWNT's used in this study were prepared using an arc discharge technique, then purified in air by heating to  $\sim 690^\circ\text{C}$ . The transport experiments described below are made possible by a technique that allows reliable electrical contacts to be fabricated to both ends of a MWNT.<sup>10</sup> Our procedure allows the electrical contacts to be made to the MWNT without the chemical processing used in conventional optical or electron-beam lithography methods. The details of this process are described elsewhere.<sup>11</sup>

An atomic force microscope (AFM) image of a typical

sample is shown in Fig. 1. Both ends of the MWNT are opened during the selection process of the nanotube for study. Since we bury both ends of the nanotube under Ti/Au contact pads, it is possible for us to simultaneously contact many layers of the MWNT. The samples studied here generally contain a rope comprised of a few ( $\sim 3-6$ ) MWNT's, as suggested from a number of AFM and transmission electron microscopy (TEM) studies. We have clear evidence that some MWNT's in these ropes are broken, and it appears likely that only a few (possibly only one) MWNT's are electrically connected to both contact pads.<sup>11</sup> These continuous MWNT's may contain a number of layers, with each layer having a different diameter and chirality. As seen in Fig. 1, for our samples there are two contacts to the MWNT. How-

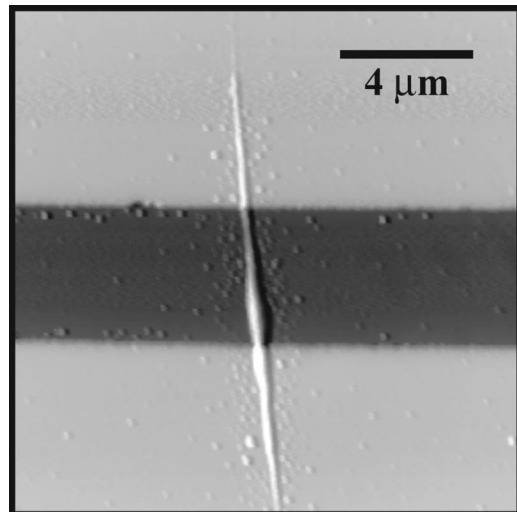


FIG. 1. An AFM image of a typical sample. The upper and lower bright regions are Ti/Au contact pads separated by  $4.3 \mu\text{m}$  and connected by a MWNT. The dark region is the glass substrate.

ever, we connect four leads to these two contact pads to acquire  $I(V)$  data as a function of temperature. The differential conductance [ $G(V, T) \equiv dI/dV$ ] is calculated by taking a numerical derivative of the data.

In all, about 100 samples of MWNT's were prepared as described above. From these samples, approximately 21 survived all steps of the fabrication process. Many of the samples failed in the early stages of this study, when the mounting techniques were still under development. In addition, we have found that samples prepared during the winter months (low humidity) have a greater chance of failure than samples prepared during the summer months (high humidity). We believe this observation points to problems associated with electrostatic discharge.<sup>11</sup>

### III. TRANSPORT MODELS

If the low-temperature conductance is dominated by ballistic transport, then one might expect that as the temperature is lowered, the conductance would increase as the amount of phonon scattering decreases. As we will show, our experimental data contradict this expectation. In an attempt to understand the temperature dependence of the conductance data, we have considered the following models: (i) thermally activated conduction,<sup>12</sup> (ii) simple two-band model appropriate for graphite,<sup>13</sup> (iii) a zero in the transmission probability induced by gap states,<sup>14</sup> (iv) variable range hopping mechanisms,<sup>15–17</sup> (v) 1D and 2D weak localization,<sup>8,9,18</sup> and (vi) Luttinger liquid behavior.<sup>5–7</sup> Of all these models, the LL model provides the most consistent explanation for the observed temperature and voltage dependence of the conductance. Schönberger *et al.* have measured MWNT conductance, which for high-conductance samples is well described by 1D weak localization and for low-conductance samples is better fit to a LL model.<sup>9</sup> All of our MWNT samples studied as a function of temperature are high conductance and best described by the LL model. The temperature dependence of the conductance is not well fit by either 1D or 2D weak localization models, but the lack of magnetotransport data at this time prevents us from excluding these models entirely. Based on our conductance values, we do not expect (nor have we observed) Coulomb blockade effects.

#### Luttinger liquid

In what follows we analyze our data in terms of the Luttinger liquid theory.<sup>19–24</sup> In a one-dimensional metal, strong Coulombic interactions between the electrons may modify the density of states (DOS) from that predicted by a Fermi liquid theory. The resulting system is a highly correlated electron liquid that is characterized by a power-law vanishing of the DOS near the Fermi energy  $E_F$ . In the event that this behavior exists, the transport through a nanotube may be described in terms of a 1D Luttinger liquid.<sup>5–7,25,26</sup> Such a system displays a power-law dependence in the electronic tunneling density of states ( $\text{DOS}_{\text{tun}}$ ) as a function of energy  $E$ . Specifically, one finds  $\text{DOS}_{\text{tun}} \propto (E - E_F)^\alpha$ .<sup>6,7</sup> This power-law suppression of the DOS gives rise to a temperature and voltage dependence in the differential conductance ( $G \equiv dI/dV$ ), given by<sup>1</sup>

$$G(V, T) = AT^\alpha |\Gamma(z)|^2 \cosh\left(\frac{x}{2}\right) \otimes \frac{1}{4k_B T} \text{sech}^2\left(\frac{E - eV}{2k_B T}\right), \quad (1)$$

where  $A$  is a constant,  $\Gamma$  is the gamma function,  $z = 1 + \alpha/2 + ix/2\pi$ ,  $x = \eta eV/k_B T$ , and  $\otimes$  represents a convolution with the thermal broadening of the electrical leads.

The multiplicative factor  $\eta$  in the definition of  $x$  accounts for the voltage division introduced by the contact of the leads to the Luttinger liquid. This factor plays a crucial role in fitting experimental data to theoretical expectations. Typically,  $\eta$  is expected to have a value of 0.5 if two tunnel barriers couple the nanotube to the contact pads (i.e., weak coupling). This is the case for which the theory was developed (i.e., *tunneling* DOS). If electrical resistance between the LL and contact pads is comparable to the nanotube resistance, then  $\eta$  may be substantially reduced from its limiting value of 0.5.

Equation (1) can be written as<sup>2</sup>

$$G_{LL}(V, T) = AT^\alpha \left| \Gamma\left(z + \frac{1}{2}\right) \right|^2 \sinh\left(\frac{x}{2}\right) \left[ \frac{1}{2} \coth\left(\frac{x}{2}\right) - \frac{1}{\pi} \text{Im} \Psi\left(z + \frac{1}{2}\right) \right], \quad (2)$$

where  $\Psi$  is the digamma function.

Equation (2) has two important limits specified by

$$G_{LL}(V, T) \propto T^\alpha \quad \text{when} \quad \frac{eV}{k_B T} \ll 1 \quad (3)$$

and

$$G_{LL}(V, T) \propto V^\alpha \quad \text{when} \quad \frac{eV}{k_B T} \gg 1. \quad (4)$$

For intermediate values of  $eV/k_B T$ , a scaling law is expected to hold.<sup>1,22–24</sup>

Depending on where the nanotube is contacted, the exponent  $\alpha$  is determined by the LL interaction parameter  $g$ . The parameter  $g$  is related to the number of conducting channels at  $E_F$  and the ratio of the charging energy of the tube to the single-particle level spacing.<sup>1,9</sup> For strong electron-electron interactions we have  $g < 1$ , while in the absence of interactions  $g = 1$  (i.e., Fermi liquid). Based on estimates for  $g$ , values for  $\alpha$  range between 0.2 and 0.6. For the specific case of a MWNT with  $N$  layers, the LL model must be modified to accommodate the multiple layers involved in screening. The resulting relationships are<sup>7</sup>

$$\alpha_{\text{end}} = \frac{1}{4N} \left( \frac{1}{g} - 1 \right), \quad (5)$$

$$\alpha_{\text{bulk}} = \frac{1}{8N} \left( \frac{1}{g} + g - 2 \right), \quad (6)$$

where the subscript *end* designates the case of electron injection into the end of a layer, and *bulk* designates the case of electron injection into the side of a layer. The effect of the electron interaction is stronger for the *end* case because the

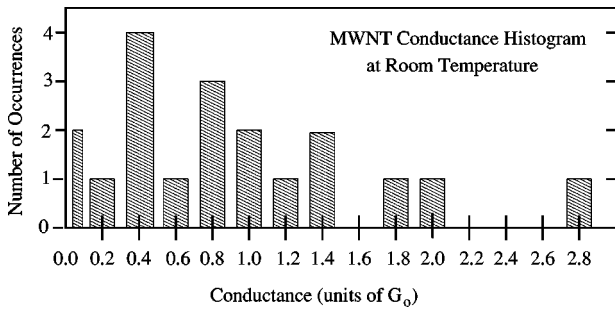


FIG. 2. A histogram of the room-temperature conductance of 19 of the 21 samples prepared for this study. Two samples having conductances greater than  $3G_0$  are not shown (Ref. 27).

electrons can only respond to an added electron by moving in one direction, whereas for the *bulk* case, the electrons can move in two directions. The above theory provides clear predictions for the behavior of a MWNT system if it is governed by a LL model.

## IV. RESULTS

### A. Conductance data

A histogram of the room-temperature conductance of 19 of the 21 samples prepared is given in Fig. 2.<sup>27</sup> There is no compelling evidence for room-temperature conductances near integer values of  $G_0 = 2e^2/h$  which would suggest a ballistic transport mechanism. This is perhaps not surprising in light of the recent results indicating transport properties can be affected by adsorbed gases.<sup>28</sup>

From the 21 samples prepared, six were selected for further study as a function of temperature. The temperature evolution of the conductance displayed similar characteristics for all of the six samples studied. Typical data taken from sample No. 29 are shown in Fig. 3. The data in this figure show five noteworthy features that are common to data obtained from all six samples studied here. These features in-

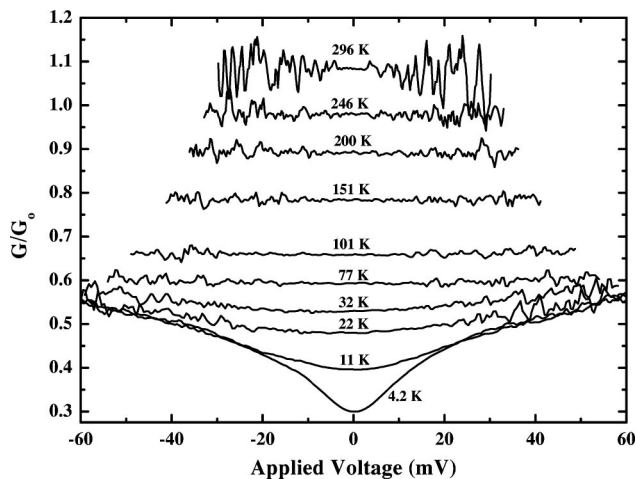


FIG. 3. The conductance  $G(V,T)$  plotted in units of  $G_0$  ( $\equiv 2e^2/h$ ) as a function of applied voltage  $V$  for sample No. 29. The data are plotted at ten different temperatures, with the temperature label adjacent to the data curve.

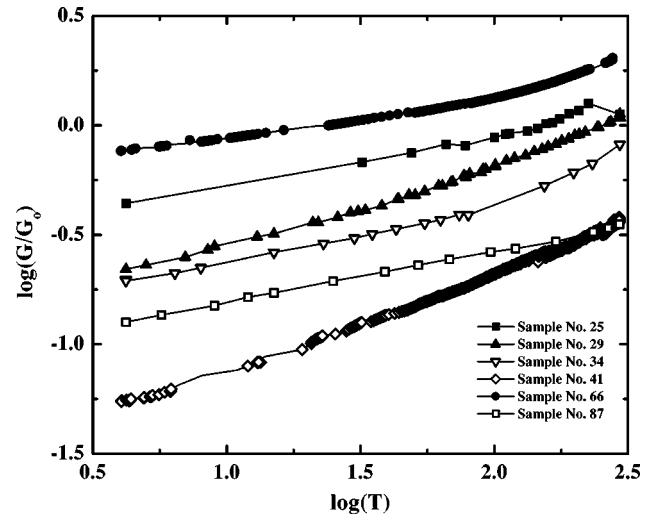


FIG. 4. A plot of  $\log[G(0,T)]$  vs  $\log(T)$  for six MWNT samples. This plot shows the power-law dependence of the zero-bias conductance. For some samples, a change in the slope of the data occurs near 100 K. The values for the slope of the data below 100 K, obtained by least-squares fits, are tabulated in Table I.

clude (i) the presence of nearly Ohmic behavior near room temperature, (ii) the appearance of a nonlinearity in  $I(V)$  which appears as a downward bow in  $G(V,T)$  at temperatures below  $\sim 20$  K, (iii) the evolution of this bow into a conductance gap which is fully developed at temperatures near 4 K, (iv) the saturation of the conductance at higher bias ( $V > 50$ – $70$  mV) for temperatures below  $\sim 20$  K, and (v) the presence of temperature- and voltage-dependent noise in the  $I(V)$  data which clearly shows up in the conductance near room temperature.

In terms of the LL model, we analyze the temperature-dependent conductance data at zero bias  $G(0,T)$  by plotting  $\log[G(0,T)]$  versus  $\log(T)$ . Figure 4 shows such a plot for all six samples. As evident from this plot, the data can be characterized by a power law of the form suggested in Eq. (3). Analysis of this data shows a change in the exponent  $\alpha$  for most of the samples studied. Least-squares fits to the data, for  $T < 100$  K, provide unbiased estimates of  $\alpha$ , which are listed in Table I.

In accordance with Eq. (2), a consequence of LL theory is that the quantity  $G(V,T)/T^\alpha$  should scale as  $eV/k_B T$ . If LL behavior is present, the scaled conductance measured as a function of voltage at different temperatures should collapse onto a universal curve.<sup>3,22</sup> The data were analyzed in this way by plotting  $G/T^\alpha$  as a function  $eV/k_B T$  for several temperatures between 4.2 K and  $\sim 30$  K, as shown for sample No. 29 in Fig. 5. For reference, the dashed line gives a plot of Eq. (2) using  $\alpha = 0.3$  and  $\eta = 0.095$ . Surprisingly, the data do not collapse onto the universal curve predicted by Eq. (2) and significant deviations are observed when  $10 \leq eV/k_B T \leq 100$ . Values of  $\eta$ , the voltage division factor, determined from similar scaling plots are collected in Table I for the other samples.

### B. Improved model

A critical reading of the previous section reveals two important features in our conductance data. First, as seen in Fig.

TABLE I. Relevant parameters for the six samples studied. <sup>a</sup>

Sample ID	Conductance		Eq. (2) fitting parameters	
	$G(V=0,300\text{ K})$	$\alpha$ ( $T < 100\text{ K}$ )	$\alpha$ ( $4KdI/dV$ )	$\eta$ (from scaling)
25 <sup>b</sup>	$1.26G_0$	0.22	0.21	–
29	$1.08G_0$	0.34	0.23	0.095
34	$0.82G_0$	0.24	0.21	$\sim 0.09$ <sup>c</sup>
41	$0.41G_0$	0.42	0.43	0.30
66	$2.03G_0$	0.17	0.12	0.07
87	$0.35G_0$	0.24	0.26	0.25

<sup>a</sup>All fitting parameters are believed accurate to  $\pm 0.02$ , a number obtained from the least-squares fitting procedure.

<sup>b</sup>Not enough low-temperature data to obtain a reliable fit.

<sup>c</sup>Fits not convincing for  $50 \leq x \leq 100$ .

5, the data do not really collapse onto the universal curve predicted by Eq. (2). The data deviate significantly in the decade of  $10 \leq eV/k_B T \leq 100$ . Second, the values of  $\eta$  obtained from this study are evidently smaller than those found in previous transport studies on SWNT's.<sup>1</sup> Bockrath *et al.* and Yao *et al.* have used the LL model to successfully describe the conductance of SWNT systems.<sup>1,2</sup> As mentioned above, Schönenberger *et al.* have interpreted some low conductance MWNT data in terms of the LL model.<sup>9</sup> One important factor is that in our case, the overall system conductance is high which we believe is due to the strongly coupled contacts produced using our fabrication technique. For the case of contacts strongly coupled to the nanotube, the contact resistance should be smaller than for weakly coupled contacts. Thus, our contact resistance to the nanotube is low and does not dominate the overall system resistance.

When the contact resistance is on the order of the nanotube resistance, there will be a significant voltage drop along the nanotube. Thus, the voltage division factor  $\eta$  of Eq. (2)

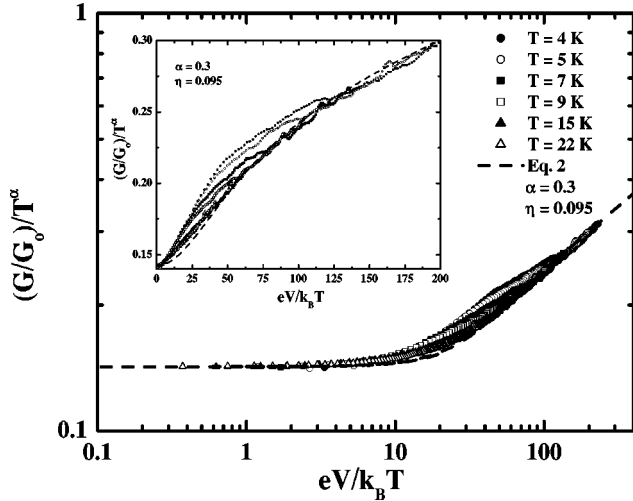


FIG. 5. A plot of  $\log[(G/G_0)/T^\alpha]$  vs  $\log(eV/k_B T)$  from the low-temperature data acquired from sample No. 29 indicating that the data roughly follow a scaling relationship. The dashed line is a plot of Eq. (2) with  $\alpha=0.3$  and  $\eta=0.095$ . The inset is a plot of the same two quantities on a linear scale and shows the deviation of the data from theory for  $10 \leq eV/k_B T \leq 100$ .

may be less than 0.5, depending on the ratio of contact resistances to nanotube resistance. This scenario was also reported by Postma *et al.* in their study of buckled and crossed SWNT's.<sup>3</sup> In their case, the voltage appears at the contacts to the nanotubes and at the buckled and crossing regions. For a SWNT junction they find a value of 0.18 for  $\eta$ .<sup>3</sup> Thus, how the voltage is divided is very important, and since our contact resistance is low, we must consider the resistance of the nanotube itself. This is illustrated schematically in Fig. 6.

For this simple picture, the total system conductance is given by

$$G_{total} = \frac{G_{NT} \times G_{LL}}{2G_{NT} + G_{LL}}, \quad (7)$$

where  $G_{LL}$  is the Luttinger liquid component of the conductance [given by Eq. (2)] and  $G_{NT}$  is the conductance of the nanotube itself. As shown in Fig. 6, the LL resistance ( $G_{LL}^{-1}$ ) is physically located at the contacts to the nanotube, where the Fermi-liquid electrons must enter the non-Fermi-liquid nanotube. The only new parameter introduced by Eq. (7) is the nanotube conductance. In fitting the low-temperature conductance data, we assume  $G_{NT}$  is a constant which is determined by a least-squares fit to data. By using the simple model of three series resistors, the constant chosen for the nanotube conductance and the value of the LL term dictate the value of the voltage division factor  $\eta$  used in Eq. (2) for  $G_{LL}$ . The total voltage drop  $V$  across the sample may be written as

$$V = 2\Delta V_{LL} + \Delta V_{NT} = 2\eta V + (1 - 2\eta)V, \quad (8)$$

where  $\Delta V_{LL} = IG_{LL}^{-1}$  and  $\Delta V_{NT} = IG_{NT}^{-1}$ . Thus,  $\eta$  is related to the ratio of the conductances by

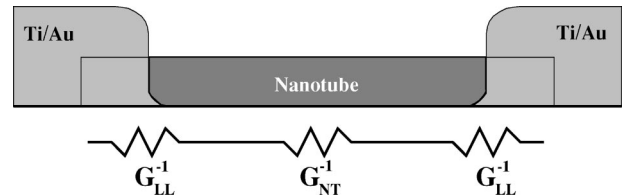


FIG. 6. A schematic illustrating the location of the resistances in our MWNT samples.

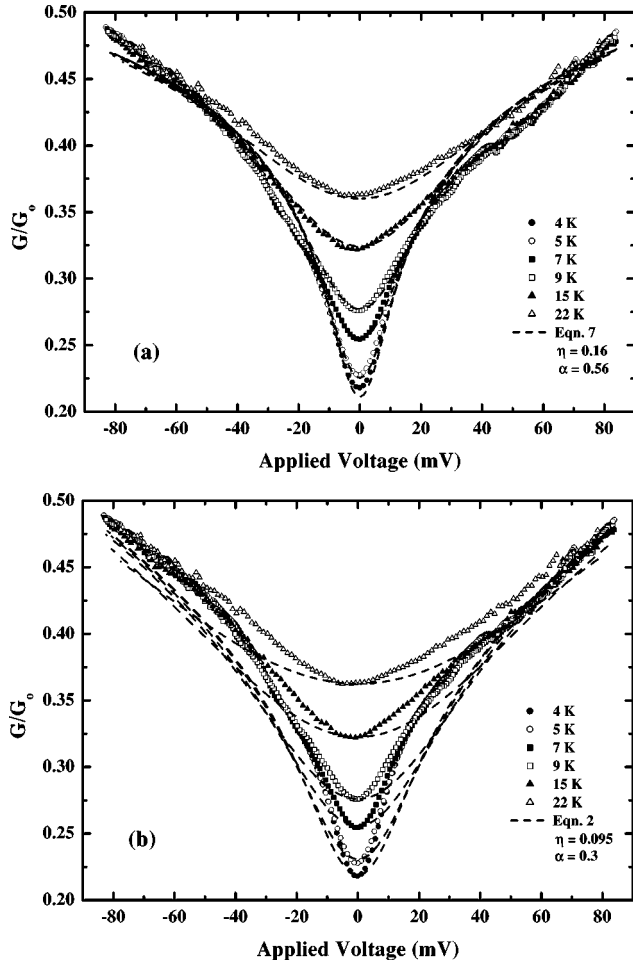


FIG. 7. A plot of  $G(V,T)$  vs voltage at six temperatures for sample No. 29. The data is shown as symbols, and the theoretically calculated curves are shown as dashed lines. In (a) we show fits using Eq. (7). For comparison, in (b) we show fits using Eq. (2).

$$\eta = \frac{1}{2 + G_{LL}/G_{NT}}. \quad (9)$$

### C. Improved fits to the data

The conductance as predicted by Eq. (7) no longer necessarily follows a power law. Also, the scaling relationship no longer holds and the theory does not predict a universal behavior for any finite values of  $G_{NT}$ . However, we can use Eq. (7) to fit the low-temperature conductance data. Fits for sample No. 29 are shown in Fig. 7(a) for the same six temperatures as in Fig. 5. Since a scaling law does not apply for Eq. (7), for comparison the fits shown in Fig. 7(b) were calculated with Eq. (2) using the same parameters as in Fig. 5. The data are shown as symbols, and the theoretical curves are dashed lines for the corresponding temperature.

The parameters used in Eq. (7) for the calculations shown in Fig. 7(a) were determined using a least-squares fitting program written in MATHEMATICA. Only the low-temperature data were fit using this procedure. For these calculations, the nanotube conductance  $G_{NT}$  was assumed constant and was

TABLE II. Fitting parameters used with Eq. (7) for the six samples studied.<sup>a</sup>

Sample ID	Conductance		Eq. (7) fitting parameters		
	$G$ ( $V=0,300$ K)	$G_{NT}$	$A$	$\alpha$	$\eta$
25 <sup>b</sup>	1.26	0.77	1.37	0.95	0.05
29	1.08	0.67	0.68	0.56	0.16
34	0.82	0.42	0.81	0.53	0.13
41	0.41	0.34	0.14	0.58	0.23
66	2.03	1.25	3.80	0.39	0.12
87	0.35	0.50	0.47	0.36	0.24

<sup>a</sup>Conductances are in units of  $G_0$ , and all fitting parameters are believed accurate to  $\pm 0.02$ , a number obtained from the least-squares fitting procedure.

<sup>b</sup>Not enough low-temperature data to obtain a reliable fit.

used in Eq. (9) to calculate  $\eta$ . Since  $G_{LL}$  is a function of  $\eta$ , we iterate Eq. (9) to find a self-consistent value for  $\eta$ .

Using a voltage- and temperature-independent  $\eta$ , the improvement in the fits to the data is remarkable. By simply adding a single component for the nanotube conductance, we are able to significantly improve the fit to the low-temperature data. The data in the region  $10 \leq eV/k_B T \leq 100$  ( $\sim 3.5$ – $35$  mV at 4 K), which departed from the LL model alone, are now well described.

Given the quality of the fits calculated for a constant value of  $\eta$ , we believe that there may be an additional voltage- and/or temperature-dependent effect, which is not included in Eq. (7). This additional effect may stem from a voltage or temperature dependence of the nanotube itself, which may partially cancel the voltage dependence of  $\eta$ . Thus, for sample No. 29 we only calculate  $\eta$  at 75 mV, which is the high-voltage range of the data. Also, the effect of  $\eta$  is reduced as the voltage goes to zero. Despite the inconsistency in the voltage dependence of  $\eta$ , we now have a natural explanation for its small value, namely, a significant voltage drop along the nanotube. Interestingly, the presence of a voltage drop along the nanotube and not only at the contacts was directly observed using Kelvin force microscopy (KFM) and ac-electrostatic microscopy (ac-EFM).<sup>29,30</sup> Voltage drops located at the contacts to a MWNT were observed. In addition, a linear decrease in the electrostatic potential profile was reported along the length of a MWNT. From the KFM data, a value of  $\eta$  was estimated to be  $0.23 \pm 0.04$ . This is similar to the values found here.

Using the same fitting procedure, we analyzed the data from the other five samples. The fitting parameters obtained from this procedure are listed in Table II.

### D. Further refinements

Since  $G_{LL}$  is a function of temperature and voltage, technically  $\eta$  should be calculated for every temperature and voltage as well. The change in  $\eta$  calculated at different temperatures is insignificant; however,  $\eta$  does change when calculated at different voltages. For this reason we have attempted to determine  $\eta$  self-consistently by allowing it to vary as a function of both temperature and voltage.

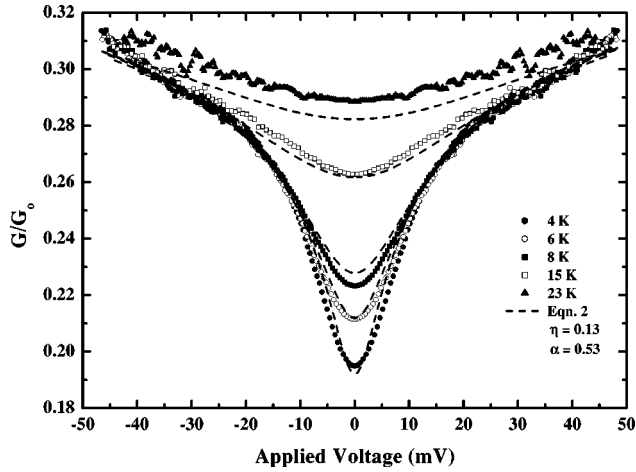


FIG. 8. A plot of conductance vs voltage for sample No. 34. The fits were calculated self-consistently with  $\eta$  determined at every voltage and temperature. The value of  $\eta$  listed was obtained by fitting the data near 45 meV at 4 K.

Attempts to fit  $G(V, T)$  from an arbitrary sample with a self-consistent  $\eta$  did not always yield good fits. We attribute this problem to the least-squares fitting routine which often would get trapped into narrow regions of parameter space while trying to optimize a particular fit. However, we performed a least-squares fit to the data from sample No. 34, with  $\eta$  calculated self-consistently at every voltage and temperature.

Figure 8 shows such a fit determined by the least-squares MATHEMATICA routine. The effect of the self-consistent determination of  $\eta$  is to produce a voltage- and temperature-dependent  $\eta$ . The value of  $\eta$  becomes larger near zero bias, where the LL term of the total conductance has its minimum. Thus, the voltage drop at the contacts becomes larger at zero bias.

As a further consistency check on this interpretation, we prepared one sample (No. 87) by placing a MWNT on *top* of the gold contacts and not buried beneath them, as was the case for the other five samples. We expect that this configuration inherently results in a poor contact to the nanotube, and indeed, this sample had the lowest zero-bias room-temperature conductance ( $0.35G_0$ ) of all six samples (see Table I). This sample displayed a clear asymmetry between the  $G(-V, T)$  and  $G(+V, T)$  data. This asymmetry may stem from poor electrical contact to the MWNT.

A similar fitting procedure using Eq. (7) as described above was carried out for sample No. 87. The low conductance dominated by the poor contacts yielded a value of  $\eta$  of 0.24, implying that  $\sim 50\%$  of the voltage was dropped at the contacts to the nanotube. In contrast, sample No. 66 yielded both the highest room-temperature system conductance and the lowest value of  $\eta=0.12$ , meaning that a total of only  $\sim 25\%$  of the voltage was dropped at the contacts to this sample. The other high-conductance samples, such as sample No. 25, also have low values for  $\eta$ . Taken all together, these observations provide further support for the correlation between the sample conductance and the coupling between the nanotube and contact, as characterized by the value of  $\eta$ .

TABLE III. Electron interaction parameters for the six samples studied, calculated from Eqs. (5) and (6) for  $N=1$ . The italicized bold entries suggest whether data from that particular sample are end or bulk contacted. All fitting parameters are believed accurate to  $\pm 0.02$ , a number obtained from the least-squares fitting procedure.

Sample ID	$g(\alpha_{bulk})$	$g(\alpha_{end})$
25 <sup>a</sup>	0.11	0.21
29	0.16	<b><i>0.31</i></b>
34	0.16	<b><i>0.32</i></b>
41	0.15	<b><i>0.30</i></b>
66	<b><i>0.20</i></b>	0.39
87	<b><i>0.21</i></b>	0.41

<sup>a</sup>Not enough low-temperature data to obtain a reliable fit.

### E. Estimates of the electron interaction parameter

The values of  $\alpha$  obtained from these improved fits can be used to estimate values of  $g$ , the electron-electron interaction parameter, using Eqs. (5) and (6). The two cases  $\alpha_{end}$  and  $\alpha_{bulk}$  are considered separately since we cannot be sure which configuration applies in each nanotube sample. The results are listed in Table III. Theoretical estimates for  $g$  typically lie around 0.18–0.3,<sup>1–3,6,7</sup> which can be compared to the data in Table III.

These estimates indicate that for sample Nos. 66 and 87, values of  $g$  calculated assuming electron injection into the sides (bulk case) of the MWNT give values close to theoretical expectations. The values of  $g$  for sample Nos. 29, 34, and 41 lie at the limits of the expected values, but are somewhat closer to the *end*-contacted case. Sample No. 25 seems also to be *end* contacted, but there is not enough low-temperature data for this sample to make a reliable estimate.

Overall, these results confirm the strong interaction effects of the electrons in the MWNT's, since all of the values for  $g$  are less than 1. In addition, all calculations have been performed assuming  $N=1$  in Eq. (6), implying that low-temperature transport through a MWNT is dominated by current flow through one shell of the nanotube.

## V. CONCLUSIONS

In summary, we measured the conductance of six MWNT samples as a function of voltage and temperature. We find that the conductance decreases roughly in accordance with a power law in temperature. The voltage dependence of the conductance at low temperatures is also well described by a power law, with the same exponent as obtained from the temperature dependence of the conductance ( $T < 100$  K). We investigated various models to explain the observed behavior of the temperature and voltage dependence. The data presented provide strong evidence for LL behavior in multi-walled carbon nanotubes. The simple model presented here describes both the voltage and temperature dependence of the nanotube conductance at low temperatures. Of all the models we have studied, the model of a Luttinger liquid in series with a contribution from the nanotube provides the

most accurate description of the observed transport behavior and a natural explanation for the small values of  $\eta$  in Eq. (2). From our analyses, estimates of the electron-electron interaction parameter  $g$  ranging between 0.1 and 0.4 are deduced. For a given sample, the value of  $g$  is consistent with theoretical estimates for electron injection into either the side (bulk) or the end of the nanotube.

The next closest temperature-dependent conductance models are weak localization or hopping conduction. Since we observe a strong voltage dependence for our samples, we believe the LL model is appropriate. The measurements of Shea *et al.* on SWNT's reveal features of weak localization and a Luttinger liquid, where the LL was distinguished by its voltage dependence.<sup>18</sup> Thus, all of the features we have mea-

sured are consistent with the LL model, with the conductance of the nanotube itself also included.

#### ACKNOWLEDGMENTS

The authors would like to thank R.P. Andres, D.B. Janes, and J. Gómez-Herrero for helpful conversations throughout the course of this work. The sample of arc-grown MWNT's was kindly supplied by R. Smalley. We would also like to thank C. Kane, C.T. White, N. Garcia, and M.P. Anantram for stimulating discussions regarding various aspects of our data. This work was partially supported by a joint U.S.-Spain Science and Technology Program (1999) Project No. 99040, by NSF Grant No. 9708107-DMR, and by ARO Grant No. DAAD19-99-1-0198.

\*Present address: Department of Materials Science & Engineering, University of Illinois at Urbana-Champaign, Urbana, IL 61801. Electronic address: elton@uiuc.edu

†Present address: IBM / Dept. 44NA, 2070 Route 52, Hopwell Jct., NY 12533.

<sup>1</sup>M. Bockrath, D. H. Cobden, J. Lu, A. G. Rinzler, R. E. Smalley, L. Balents, and P. L. McEuen, *Nature (London)* **397**, 598 (1999).

<sup>2</sup>Z. Yao, H. W. Ch. Postma, L. Balents, and C. Dekker, *Nature (London)* **402**, 273 (1999).

<sup>3</sup>H. W. Ch. Postma, M. de Jonge, Z. Yao, and C. Dekker, *Phys. Rev. B* **62**, R10 653 (2000).

<sup>4</sup>M. F. Lin, D. S. Chuu, and K. W.-K. Shung, *Phys. Rev. B* **56**, 1430 (1997).

<sup>5</sup>R. Egger and A. O. Gogolin, *Phys. Rev. Lett.* **79**, 5082 (1997).

<sup>6</sup>C. Kane, L. Balents, and M. P. A. Fisher, *Phys. Rev. Lett.* **79**, 5086 (1997).

<sup>7</sup>R. Egger, *Phys. Rev. Lett.* **83**, 5547 (1999).

<sup>8</sup>L. Langer, V. Bayot, E. Grivei, J-P. Issi, J. P. Heremans, C. H. Olk, L. Stockman, C. Van Haesendonck, and Y. Bruynseraede, *Phys. Rev. Lett.* **76**, 479 (1996).

<sup>9</sup>C. Schönberger, A. Bachtold, C. Strunk, J.-P. Salvetat, and L. Forró, *Appl. Phys. A: Mater. Sci. Process.* **69**, 283 (1999).

<sup>10</sup>P. J. De Pablo, E. Graugnard, B. Walsh, R. P. Andres, S. Datta, and R. Reifengerger, *Appl. Phys. Lett.* **74**, 323 (1999).

<sup>11</sup>E. Graugnard, R. Reifengerger, B. Walsh, and P. J. de Pablo, in *Cluster and Nanostructure Interfaces*, edited by P. Jena, S. N. Khanna, and B. K. Rao (World Scientific, Singapore, 2000), pp. 123-130.

<sup>12</sup>Neil W. Ashcroft and N. David Mermin, *Solid State Physics* (Holt, Rinehart and Winston, New York, 1976).

<sup>13</sup>L. Langer, L. Stockman, J. P. Heremans, V. Bayot, C. H. Olk, C. Van Haesendonck, Y. Bruynseraede, and J-P. Issi, *J. Mater. Res.* **9**, 927 (1994).

<sup>14</sup>M. P. Anantram, J. Han, and T. R. Govindan, in *Molecular Electronics: Science and Technology*, edited by A. Aviram and M. Ratner (New York Academy of Sciences, New York, 1998), Vol. 852.

<sup>15</sup>B. I. Shklovskii and A. L. Efros, *Electronic Properties of Doped Semiconductors*, Vol. 45 of *Springer Series in Solid-State Sciences* (Springer-Verlag, Berlin, 1984).

<sup>16</sup>H. Kamimura and H. Aoki, *The Physics of Interacting Electrons in Disordered Systems* (Clarendon Press, Oxford, 1989).

<sup>17</sup>O. E. Omel'yanovskii, V. I. Tsebro, O. I. Lebedev, A. N. Kiselev, V. I. Bondarenko, N. A. Kiselev, Z. Ja. Kosakovskaja, and L. A. Chernozatonskii, *JETP Lett.* **62**, 503 (1995).

<sup>18</sup>H. R. Shea, R. Martel, and Ph. Avouris, *Phys. Rev. Lett.* **84**, 4441 (2000).

<sup>19</sup>Johannes Voit, *Rep. Prog. Phys.* **57**, 977 (1995).

<sup>20</sup>H. J. Schulz, in *Proceedings of Les Houches Summer School LXI*, edited by E. Akkermans, G. Montambaux, J. Pichard, and J. Zinn-Justin (Elsevier, Amsterdam, 1995), p. 533.

<sup>21</sup>H. J. Schulz, G. Cuniberti, and P. Pieri, *Field Theories for Low-Dimensional Condensed Matter Systems: Spin Systems and Strongly Correlated Electrons*, edited by G. Morondi, P. Sodano, A. Tagliacozzo, and V. Tognetti (Springer, Berlin, 2000).

<sup>22</sup>A. M. Chang, L. N. Pfeiffer, and K. W. West, *Phys. Rev. Lett.* **77**, 2538 (1996).

<sup>23</sup>A. Yacoby, H. L. Stormer, N. S. Wingreen, L. N. Pfeiffer, K. W. Baldwin, and K. W. West, *Phys. Rev. Lett.* **77**, 4612 (1996).

<sup>24</sup>M. Grayson, D. C. Tsui, L. N. Pfeiffer, K. W. West, and A. M. Chang, *Phys. Rev. Lett.* **80**, 1062 (1998).

<sup>25</sup>A. Odinstsov and H. Yoshioka, *Phys. Rev. B* **59**, R10 457 (1999).

<sup>26</sup>H. Yoshioka and A. Odinstsov, *Phys. Rev. Lett.* **82**, 374 (1999).

<sup>27</sup>Two samples have been intentionally left out of the histogram. At room temperature the conductances were  $4.4G_0$  and  $27.0G_0$ . Also, sample No. 87 has a different contact configuration from the other samples, as discussed in the text.

<sup>28</sup>G. U. Sumanasekera, C. K. W. Adu, S. Fang, and P. C. Eklund, *Phys. Rev. Lett.* **85**, 1096 (2000).

<sup>29</sup>B. Walsh, MS thesis, Purdue University, 2000.

<sup>30</sup>A. Bachtold, M. S. Fuhrer, S. Plyasunov, M. Forero, Erik H. Anderson, A. Zettl, and Paul L. McEuen, *Phys. Rev. Lett.* **84**, 6082 (2000).